Targeted Drug Delivery Using Iron Oxide Nanoparticles

Introduction

In targeted drug delivery, the drug is released only within a targeted area of the body. Therefore the therapeutic effect in diseased cells and/or tissues is maximized while side effects on normal tissues are minimized. Because of their unique pharmacokinetic properties, nanoparticles have a prolonged circulation time due to the fact that they are too large to be excreted by the kidneys in a short time, yet are small enough to avoid uptake by the reticuloendothelial system within the liver or spleen. Additionally, it has been shown that tumor vasculatures are not well developed, which allows nanoparticles with sizes smaller than 100 nm to pass through the endothelial cell layer and enter into the tumor mass. Delivery of therapeutic agents using nanoparticles offers a chance to improve the water solubility and bioavailability of hydrophobic drugs. Furthermore, because of their large surface area and diverse surface chemistry, nanoparticles can potentially be employed to combine drug therapies and facilitate the delivery of several distinct drugs simultaneously to a diseased tissue. Targeting ligands can also be conjugated to the nanoparticle surface to facilitate selective and efficient delivery of drugs. Here we present uPAR-targeted IO-Dox (doxorubicin) nanoparticles can deliver higher levels of Dox into breast cancer cells and produce a stronger inhibitory effect on tumor cell growth.

Materials:

Ocean's iron oxide particle SHP10 (-COOH surface groups, 10 nm in size), conjugation kit (ICK-10), recombinant ATF (amino-terminal fragment of the high affinity receptor binding domain of urokinase-type plasminogen activator (uPA)); Doxorubicin HCl (Polymed Therapeutics, Houston, TX); mouse mammary carcinoma cell line 4T1; human breast cancer cell line MDA-MB-231.

Procedures:

1. **Conjugation of ATF to IO particles:** Conjugate ATF to SHP10 using ICK kit according to the instruction. The SHP to ATF molar ratio was 1:20. The conjugates were purified by a spin column with molecular weight cutoff of 100K (Pall Corp.)
2. **Encapsulation of Dox onto IO nanoparticles:** Dox was dissolved in methanol and then added to IO nanoparticles at a ratio of 1 mg Dox to 3 mg of iron (Fe). After rotating at room temperature for 4 hrs, free Dox was separated from the encapsulated Dox using Nanosep 100 k column filtration.
3. **pH sensitive drug release in solution:** 10 ul of various IO-Dox nanoparticles were placed in 100 ul of PBS buffer with pH 4, 5, 6, or 7. After incubating at 37°C for 2 hrs, free Dox molecules in the buffer were separated from the IO nanoparticles using Nanosep 100 k column filtration. Dox fluorescence intensity in the solution was measured and the amount of free Dox was calculated from the

Dox-only standard curve. The percentage of drug release was obtained using the total amount of Dox from input IO-Dox nanoparticles as 100%.

4. **Cell proliferation assay:** 3×10^3 of mouse mammary tumor 4T1 and human breast cancer MDA-MB-231 cells were plated in 96-well culture plates for overnight. The culture medium was then replaced with serum free medium containing IO-Dox or ATF-IO-Dox nanoparticles at a Dox concentration of 0.25 or 0.5 uM. Control groups were treated with non-targeted or targeted IO nanoparticles without Dox but have equal concentration of the IO nanoparticle as ATF-IO-Dox, or with 0.25 or 0.5 uM of free Dox. Cells were incubated with above mentioned agents for 2 hrs at 37°C in 5% CO_2 tissue culture incubator. After replacing the culture medium and IO nanoparticles with fresh culture medium, the cells were cultured for 48 hrs and then examined using inverted fluorescence microscope to determine the presence of Dox fluorescence in the cells. The percentage of tumor cell growth inhibition was determined by crystal violet cell proliferation assay. Briefly, the cells were fixed in 96 well plate using 4% formaldehyde in PBS for 20 min and then washed with PBS. 0. 5% crystal violet in H_2O was added to the wells for 20 min and unstained dye was washed away with H_2O. After air-dry, 100 ul of Sorenson's solution containing 30 mmol/L sodium citrate, 0.02 mol/L HCl, and 50% ethanol at room temperature for 20 min was added to the well to elute the dye, and the optical density was read at 590 nm using a microplate reader (SpectroMax, Molecular Devices). Absorbance value was normalized to the value of the control cell group without treatment to obtain the percentage of viable cells. Each treatment group was performed in triplicate and similar results were obtained in three separate experiments.
5. ***In vitro* MRI scan:** Human breast cancer MDA-MB-231 cells were incubated with serum free medium containing 20 pmol of ATF-IO or ATF-IO-Dox nanoparticles at 37°C for 2 hrs. After washing with PBS buffer, the cell pellets were placed in 200 ul PCR tubes and then scanned on a 4.7T MRI scanner (Philips Medical Systems, Bothell, WA) using a multi-echo T_2 weighted fast spin echo sequence which simultaneously collects a series of data points at different echo times (TE_i, $i = 6$) for T_2 relaxometry measurement. T_2 relaxation time of each sample was calculated by fitting the decay curve of MRI signals (M_i) over different TE points on a pixel-by-pixel basis using the non-linear mono-exponential algorithm of $M_i = M_0 * \exp(-TE_i/T_2)$.

Results and Discussions

Loading efficiency of Dox onto IO nanoparticles

Our drug loading approach takes advantage of hydrophobic interaction between the hydrophobic inner layer of the IO nanoparticles and the hydrophobic drug molecules. We found that Dox can be efficiently incorporated onto the amphiphilic block polymer coated IO nanoparticles by simply mixing the IO nanoparticles with appropriate concentrations of Dox. We found that a Dox to IO (Fe) ratio of 1 mg Dox: 3 mg of Fe results in IO-Dox nanoparticles with a high level of encapsulated Dox molecules while avoids aggregation of particles at a high Dox concentration. Using this method, over 95% (10 nm IO) of added Dox were incorporated onto the IO nanoparticles. Additionally, it seems that

surface modification affects the efficiency of Dox encapsulation. Conjugation of ATF peptides to the surface of the IO nanoparticles also decreases the drug encapsulation by 26% (Table I).

Table I. Encapsulation efficiency of Dox in IO nanoparticles with surface modifications.

Drug encapsulation	SHP10-Dox	ATF-SHP10-Dox
Numbers of Dox per IO particle	652±253	480±71
Percentage of IO (weight%)	2.3±0.73	1.7±0.25
Percentage of Fe^{2+} (weight%)	21±6.7	15.6±2.3

pH sensitive release of Dox from IO nanoparticles

One of the most important aspects for a drug delivery vehicle is its ability to release the payload drug efficiently into cells at the target. The amine group of Dox may facilitate its conversion to a charged molecule at low pH and becomes soluble in water. Therefore, we examined whether Dox can be released from IO nanoparticles in acidic pH, which resembles pH of intracellular vesicles such as endosomes (pH 5.5 – 6.0) and lysosomes (pH 4.5 – 5.0). Our result shows that Dox molecules can be efficiently released from the non-targeted or uPAR-targeted ATF-IO-Dox nanoparticles under acidic conditions after 2 hr incubation. Incubation of above nanoparticles in pH 6.0 buffer enables the release of 20 – 30% of Dox molecules from the drug loaded nanoparticles (Fig.1). At pH 5.0, 30-40% of encapsulated Dox were released from the nanoparticles. Furthermore, under pH 4.0 conditions, about 70 to 80% of encapsulated Dox were released into the buffer (Fig.1). Importantly, conjugation of ATF peptides to IO nanoparticles did not affect the drug release efficiency (Fig.1).

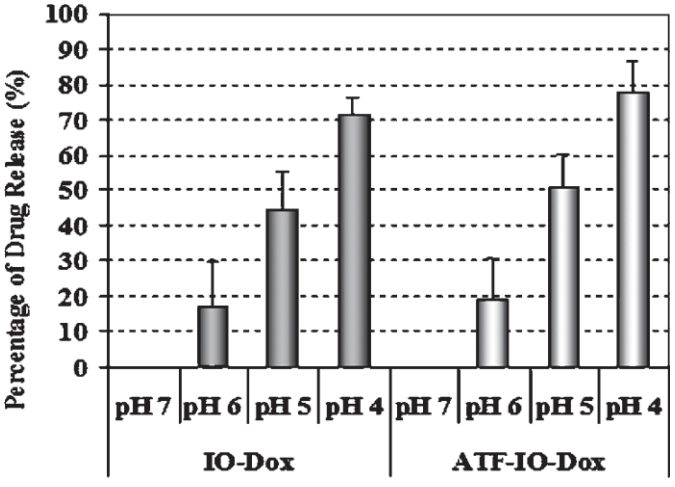

Fig. 1. Examination of pH sensitive release of Dox from non-targeted or ATF-targeted IO nanoparticles *in vitro* Non-targeted and targeted-IO-Dox nanoparticles containing 400 to 600 pmol of Dox were placed in the buffer with pH 4, 5, 6 and 7 for 2 hrs at 37°C. The amount of released Dox molecules was determined by measuring fluorescence intensity in solution and then calculated from the Dox standard curve. The total amount of Dox added to IO-Dox or ATF-IO-Dox nanoparticles is used as 100%. Result shown is the mean of three repeat experiments.

uPAR-targeted IO-Dox nanoparticles produce a strong cytotoxic effect on breast cancer cell lines

To evaluate the feasibility of the targeted IO-Dox nanoparticles for the treatment of breast cancer, we examined the cytotoxic effect of the targeted or non-targeted IO-Dox nanoparticles on MDA-MB-231 and 4T1 cell lines. We incubated the cells with free Dox, IO-Dox or ATF-IO-Dox nanoparticles for 2 hrs, which allows for uPAR-targeted IO nanoparticles to be internalized by cells. The culture medium was then replaced with fresh medium and the cells were cultured without additional treatment for 48 hrs. We found that ATF-IO nanoparticles deliver a much higher level of Dox into tumor cells, compared to the equal concentration of free Dox or IO-Dox treated cell groups. For example, treatment of 4T1 cells with 0.5 uM of free Dox or non-targeted IO-dox did not show the accumulation of Dox fluorescence nor any cytotoxic effects on the cells (Figs.2(A and B)). However, strong Dox fluorescence was detected in the cells treated with 0.25 to 0.5 uM of ATF-IO-Dox nanoparticles (Fig.2(A)). High magnification fluorescence image shows that Dox fluorescence is located in the cell nucleus. A marked inhibition of tumor cell growth was also found in ATF-IO-Dox nanoparticle treated cells (Fig.2(B)). Similarly, 0.5 uM of free Dox did not induce death of human breast cancer cells. A low level of non-targeted IO-Dox was seen in MDA-MB-231 cells after 2 hr incubation, causing 50% of growth inhibition in the cells (Figs.2(C and D)). However, over 90% of growth inhibition of MDA-MB-231 cells was detected after treating the cells with 0.25 to 0.5 uM of Dox in ATF-IO-Dox nanoparticles. Our results demonstrate that the receptor targeted IO nanoparticles have a high efficiency in delivery of payload drugs into tumor cells to produce a strong anti-tumor effect.

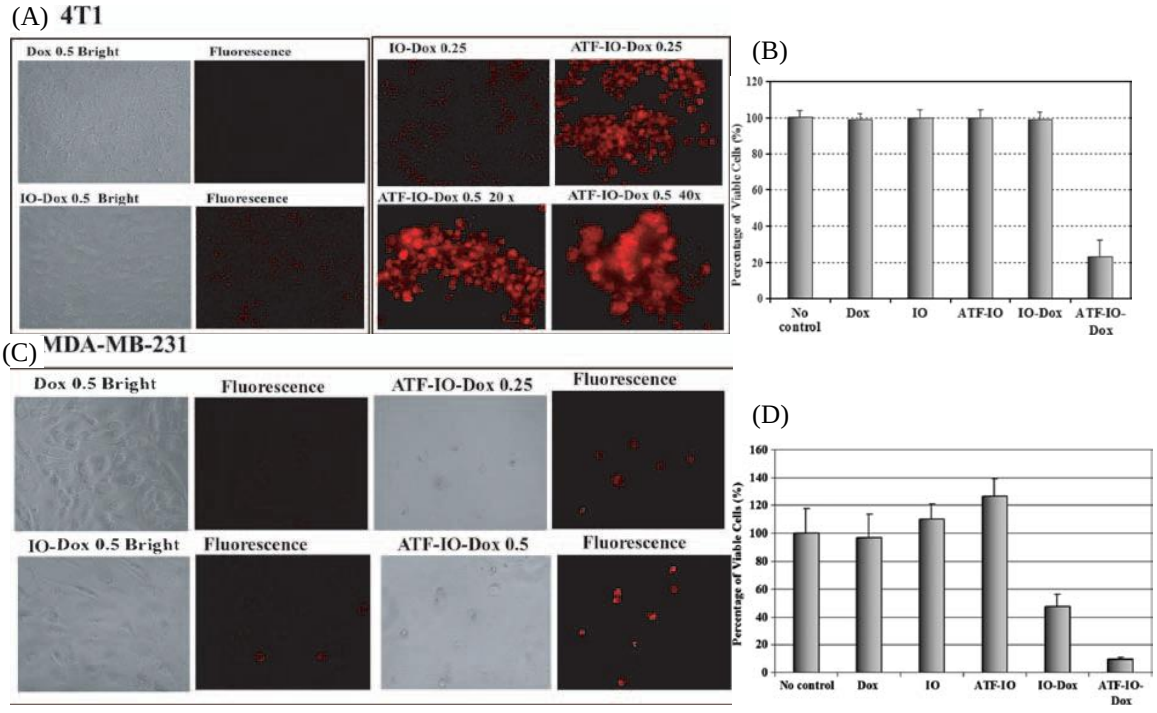

Fig. 2. Detection of effect of drug delivery using ATF-IO-Dox on breast cancer cells *in vitro*. Cells cultured in 96 well plates were incubated with the medium containing 0.25 or 0.5 uM of free Dox, IO-Dox or ATF-IO-Dox nanoparticles as well as control IO and ATF-IO nanoparticles for 2 hrs. IO nanoparticles with 10 nm core size were used from this study. After removing the drug and nanoparticles, the cells were cultured for 48 hrs and then fixed with 4% formaldehyde in PBS buffer. A and B: Examination of the viable cells and Dox fluorescence in 4T1 cells using phase contrast and fluorescence microscopy and cell proliferation assay. Treatment of the cells with 0.5 uM of free Dox and IO-Dox nanoparticles did not induce cell death in 4T1 cells. Dox fluorescence was absent or present in a very low level in those cells (A). However, a high level of Dox was detected in the tumor cells after 0.25 to 0.5 uM of ATF-IO-Dox treatment. Higher magnification fluorescence image (40× lens) shows the presence of Dox in the cell nucleus. Cell proliferation assay shows that treatment of 4T1 cells with ATF-IO-Dox nanoparticles at 0.5 uM of Dox concentration induces cell death in 75% of the cells, while the same drug concentration of free Dox or IO-DOX, or same IO concentration of IO or ATF-IO treated cells did not show any cytotoxic effects on the cells (B). In human breast cancer MDA-MB-231 cells, 0.5 uM of free Dox treatment did not induce cell death and Dox fluorescence was not detected in the cells (C and D). Our result showed non-specific uptake of IO-Dox by MDA-MB-231 cells also induced cell death. However, a higher level of Dox fluorescence and 40% more cell death were found in ATF-IO-Dox treated cells compared to IO-Dox treated cells (C and D). A slightly high percentage of MDA-MB-231 cells detected in ATF-IO treated group is due to the internalization of IO nanoparticles into cells resulting in an enhanced Crystal Violet staining. Results shown are the mean of four repeat samples. Similar results were obtained from three separate studies.

Encapsulation of Dox molecules onto ATF-IO nanoparticles does not affect T_2 contrast of the IO nanoparticle

A major goal of our research is to develop multifunctional nanoparticles for simultaneous drug delivery and tumor imaging. Our preparation of IO nanoparticles has strong T_2 shortening effect that leads MRI signal drop or "darken" contrast using T_2 weighted imaging. To determine the feasibility of using IO-Dox nanoparticles as a MRI contrast agent, we examined MRI contrast effect of ATF-IO-Dox nanoparticles. MDA-MB-231 cells were incubated with ATF-IO or ATF-IO-Dox nanoparticles for 2 hrs and unbound nanoparticles were washed away by centrifugation. Results from MR imaging of ATF-IO-Dox or ATF-IO nanoparticle treated cell pellets showed that the ATF-IO-Dox labeled cells have a similar T_2 value as the cells labeled with ATF-IO particles without Dox (Fig.4(A)). T_2 values in ATF-IO or ATF-IO-Dox labeled cells were four times lower than that of unlabeled cells, suggesting that ATF-IO-Dox nanoparticles can be used as a targeted drug delivery vehicle as well as a MRI contrast agent.

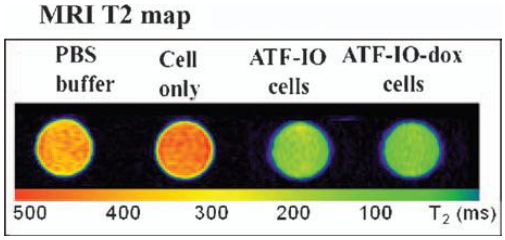

Fig. 3. Effect of drug encapsulation on the T_2 weighted MRI contrast produced by IO nanoparticles. Human breast cancer MDA-MB-231 cells were incubated with 20 pmol of ATF-IO or ATF-Dox-IO nanoparticles for 4 hrs. After washing with PBS, the cell pellets were examined using 4.7T MRI scanner. MRI T_2 relaxometry demonstrated that ATF-IO and ATF-IO-Dox labeled tumor cells have similar T_2 values of 112±10 and 118±10 ms, respectively. However, T_2 value in ATF-IO or ATF-IO-Dox labeled cells is three times lower compared to unlabeled cells (470±10 ms), suggesting that ATF-IO-Dox nanoparticle may be used as a targeted MRI contrast agent. Echo time (*TE*) has a unit in million seconds as shown in the figure. Orange-red color in the scale bar indicates a high T_2 value and green color represents a low *T* value.